One- and two-electron capture in collisions of slow B^{4+} and Be^{4+} ions with helium

Wolfgang Fritsch
Bereich Schwerionenphysik, Hahn-Meitner-Institut Berlin, D-1000 Berlin 39, Germany

C. D. Lin
Department of Physics, Kansas State University, Manhattan, Kansas 66506
(Received 6 September 1991)

One-electron and two-electron capture in slow B^{4+}-He and Be^{4+}-He collisions are studied within the semiclassical close-coupling description with two-electron atomic basis sets. For B^{4+}-He collisions, we find large two-electron capture cross sections to $2l2l'$ doubly excited projectile states. Double-capture cross sections to $2s^2\,{}^1S^e$, $2s2p\,{}^1P^o$, and $2p^2\,{}^1D^e$ states and the relative M distributions are found to be in good agreement with recent experiments. Earlier data on B^{3+} production are found to contain large portions of double transfer followed by autoionization. For the Be^{4+}-He system, the summed cross sections from this work agree with an earlier theoretical study within the adiabatic model. Discrepancies remain, however, for this system in the distribution of double transfer over final states.

PACS number(s): 32.80.Dz, 34.70.+e, 34.10.+x

INTRODUCTION

In atomic collisions at low energies, the dynamics of a single electron is well described within the standard framework of the semiclassical close-coupling method [1]. Formally, this description can also be used for the dynamics of two active electrons. In practice, however, serious problems may occur: (1) the large number of two-electron configurations is very hard to accommodate in the close-coupling framework, and (2) interferences between resonance states and the continuum cannot be treated adequately in present-day formulations [1]. It is therefore only in a few cases that two-electron transitions to bound states have been analyzed in the two-electron formulation of the close-coupling description, cf. the discussion in Ref. [1].

In this work we deal with the capture of one or two electrons in slow collisions of B^{4+} and Be^{4+} with helium atoms. It is well known that two-electron capture can become an important channel in slow atomic collisions, or indeed the dominant channel in resonant He^{2+}-He collisions [1,2] or in C^{4+}-He collisions [1,3]. This work is hence intended to broaden our knowledge about such low-energy processes, by considering projectiles which have found no (B^{4+}) or little (Be^{4+}) [4] attention by theorists to date. In these systems, two-electron capture populates predominantly doubly excited states. These states autoionize with the emission of electrons. Measurement of the angular distribution of these electrons provide the M dependence of the population of doubly excited states [5,6]. If only projectile charge states are analyzed, these doubly excited states contribute to the yield of single-capture events. Clearly, these particular collision systems are of major interest for applications [7], given the abundance of beryllium and boron ions in plasmas of newly designed fusion devices. This work has, however, been inspired first by the possibility [5] to measure the M dependence of the population of doubly excited states in two-electron capture, and by the planned extension [6] of such measurements of the B^{4+}-He system.

THEORY

In the following we will discuss the theoretical description of the B^{4+}-He collision system first. The $1s$ core electron in the projectile will be considered inert; it will be represented by taking a screened potential for the B^{4+} ion. The Be^{4+}-He collision is simpler in that its projectile does not carry an extra electron. The main weight of this investigation is still on the B^{4+}-He system because it is easier to access experimentally. The Be^{4+}-He system has been already investigated [4] within the molecular-orbital close-coupling model.

From available information for the isocharged C^{4+}-He system [3] one expects that one-electron transfer in B^{4+}-He and Be^{4+}-He collisions leads predominantly to the population of the $n=2$ shell of the projectile. A naive independent-particle picture then suggests that two-electron transfer populates mainly the $2l2l'$ projectile states. A minimal atomic-orbital (AO) basis set for the close-coupling description [1,8] would hence consist of representations of these states: (i) the initial $1\,{}^1S$ He ground state, (ii) the one-electron transfer states which are products of $2s$ and $2p$ B^{3+} orbitals with the $1s$ He^+ orbital, and (iii) the two-electron transfer states $2l2l'$ of B^{2+}. Note that in this and in the following discussion, the $1s$ core electron is dropped from the explicit specification of capture states of the B^{4+} projectile.

The initial ${}^1S$ He ground state has been written as a superposition of a $1s(\zeta)1s(\zeta')$ and a $2p(\hat{\zeta})2p(\hat{\zeta}')({}^1S)$ state, where the charge parameters $(\zeta,\zeta',\hat{\zeta},\hat{\zeta}')$ of the hydrogenic orbitals $[1s(\zeta),\ldots,2p(\hat{\zeta}')]$ have been determined by minimizing the ${}^1S$ He energy. All two-electron configurations have been properly antisymmetrized; they also have been assigned plane-wave translation factors which derive from their respective movement with respect to the origin of the coordinate system [8].

For the potential of the B^{4+} ion we have taken a pseudopotential of the form

$$V_p(r) = -1/r[4 + \exp(-\alpha r)(1+\beta r+\gamma r^2)] , \quad (1)$$

with $\alpha=\beta=10$ and $\gamma=50$ in atomic units. The screening function in this potential is somewhat different from the screening which would be caused by the frozen-electron distribution of one electron in the B^{5+} $1s$ shell, but the energies of one-electron and two-electron states in potential (1) are found to be close to the experimental energies, cf. below.

With this potential V_p, we have determined single-capture states in B^{4+}-He collisions as one-electron states of the potential V_p. Similarly, two-electron-capture states are determined as two-electron states of the potential V_p. Wave functions which represent single-capture states have been constructed from the set of hydrogenic orbitals given in Table I. They consist of representations of the $n=2$ B^{3+} states and some pseudostates which have been kept in the calculations. Note that the wave function with the lowest energy cannot be considered a realistic representation of the B^{3+} ground state, because the $1s$ core electron cannot be assumed to stay inert after the capture of another electron into the projectile K shell. Some test calculations also include the $n=3$ B^{3+} capture states.

Representations of two-electron capture states have been constructed with similar methods as given in Ref. [10]. Basically, the $1snl$ ($nl=1s,\ldots,2p,3s$) B^{2+} wave functions have been the first to be fixed by optimizing the charge parameters in the hydrogenic orbitals of the atomic basis. Subsequently the $2l2l'(^1L)$ wave functions have been constructed by the same optimization procedure. Of course, the calculated $1snl$ wave functions themselves cannot be expected to be realistic representations of double-capture states because the additional core electron of the B^{4+} projectile does not stay inert after the capture of a $1s$ electron. The $1snl$ wave functions are still needed in the model description of double capture in order to avoid a variational collapse of the $2l2l'$ wave functions. The details of all these basis orbitals are given in Table II. We do not give the amplitudes of the various hydrogenic components because they come out in the straightforward diagonalization procedure of the B^{2+} Hamiltonian.

TABLE I. Parameters ($nl\zeta$) of hydrogenic orbitals used to construct the single-particle states of B^{3+}. All m substates for a given l shell are included in the calculations. Energies are obtained by diagonalizing the Hamiltonian V_p, cf. text, in the space of basis functions; they are given with respect to the B^{4+} ion. The last column contains experimental $2S$ and $2P$ energies [9].

n	l	ζ	Energy (a.u.)	Expt. (Ref. [9])
1	0	5.22	−10.941	
2	0	4.305	−2.255	−2.233
2	1	4.64	−2.067	−2.053
1	0	3.19	−0.249	
1	0	2.152	13.84	
2	1	3.37	−0.559	

For an illustration of the collision dynamics, a molecular-energy diagram is useful. For one-electron systems, this can be easily constructed by diagonalizing the two-center Hamiltonian in the space of basis orbitals; for an example of this procedure with atomic basis orbitals see Ref. [12]. For two-electron systems, such energy curves may well show structures which result from variational collapse of molecular orbitals, and which impede the purpose of illustration. We have hence produced an approximate energy diagram in two steps. (1) The molecular-energy curves associated with the initial state and the one-electron transfer states have been constructed by diagonalizing a *one-electron* two-center Hamiltonian, with a one-electron basis analogous to the one given in Table I and the effective Hamiltonian of the He^+ target taken from Ref. [13]. In order to relate these energies to energies of two-electron configurations, they have been decreased by 2 a.u., the energy of the $1s$ He^+ state. (2) The energy curves associated with two-electron transfer states have been determined by diagonalizing the two-electron, two-center Hamiltonian in the space of the two-electron transfer states only. In this way the correct long-range behavior of these energy curves is secured. No attempt has been made to improve the behavior of the energy curves at small interatomic separations.

Figure 1 shows the Σ states of such an approximate molecular diagram where the visual appearance of the topology has been improved by showing an effective principal quantum number n_0 [14] instead of the binding energy E of states directly. The state denoted 4Σ correlates to the initial He ground state. It is clear that this state will populate the single transfer $n=2$ B^{3+} states via a radial coupling mechanism around 3 a.u. separation, and actually to a lesser extent the $n=3$ B^{3+} states via a

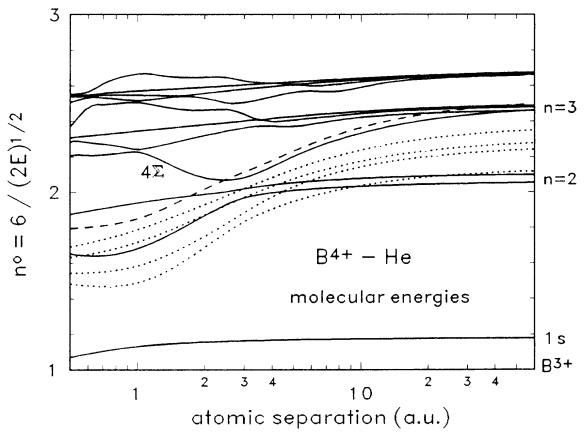

FIG. 1. Approximate molecular-energy diagram for the B^{4+}-He collision systems. Only Σ states are shown. The solid lines correlate, at infinite atomic separations, to the single-capture states, except the state denoted 4Σ which correlates to the He ground state. The dotted lines correlate, in the order of decreasing binding energy, to the $2s^2$, $2s2p$, $2p^2(^1D)$, and $2p^2(^1S)$ Be^{2+} double-capture states, the dashed line to the $2s3s$ Be^{2+} state. For details concerning this diagram, see text.

TABLE II. Parameters $(n_1 l_1 \zeta_1, n_2 l_2 \zeta_2)$ of hydrogenic orbitals used to construct representations of double-capture states in B^{4+}-He collisions, cf. text. L is the total angular momentum in the angular-momentum coupling of states; energies are total binding energies with respect to the B^{4+} ion. The last column contains energies of doubly excited B^{2+} configurations from Ref. [11].

n_1	l_1	ζ_1	n_2	l_2	ζ_2	L	Energy (a.u.)	Expt. (Ref. [11])	
1	0	5.689	1	0	3.8325	0	−18.86		
1	0	5.262	2	0	3.697	0	−12.26		
1	0	5.102	2	1	3.055	1	−12.07		
1	0	5.060	3	0	3.511	0	−11.49		
2	0	4.395	2	0	4.395	0	−3.939	−3.842	$2s^2\,^1S$
2	1	3.727	2	1	3.727	0	−3.184	−3.242	$2p^2\,^1S$
2	0	5.873	2	1	3.348	1	−3.513	−3.501	$2s2p\,^1P$
2	1	4.654	2	1	2.992	2	−3.404	−3.419	$2p^2\,^1D$
1	0	1.043	1	0	1.043	0	−0.590		
2	0	3.17	2	1	4.18	1	−1.610		

rotational-coupling mechanism at smaller separations (Π states link the set of $n=3$ B^{3+} states with the 4Σ state at small separations; see the analogous one-electron correlation diagram for the Li^{3+}-H system [14]). Figure 1 also shows that energy separations are favorable for the population of the set of $2l2l'$ states either directly from the initial state or from the single-capture states. In Fig. 1 there is also the curve correlating to the $2s3s$ B^{2+} state. The basis state corresponding to that particular curve is not included in the dynamical calculations. This curve is shown here to help remember that also the $2l3l'$ states are populated in the collisions though with a smaller probability.

For the Be^{4+}-He system, the projectile potential is simply the Coulomb potential of four charge units and hence the single-capture states can be included directly instead of merely by representation. In most of the calculations, only the $n=2$ Be^{3+} single-capture states have been included in the basis, while only at one energy point has the influence of the $n=3$ Be^{3+} states been tested. The double-capture states have been included, in similar ways as given above for the B^{4+}-He system, with basis states only slightly different from the states given in Table II.

We do not show an energy diagram for the Be^{4+}-He system. Its topology is not different from the one given in Fig. 1. The main difference is that the $2s$ and $2p$ capture states are now degenerate at infinite separations and still close to each other in the critical coupling region of 2–4 a.u. Also the two-electron capture states are now less bound with the biggest difference concerning the $2s^2$ state. For a more rigorous molecular diagram of the Be^{4+}-He system, see the work by Martín, Riera, and Yáñez [4] who, however, show only two Σ energy curves out of the set of four which correlate to the full set of $2l2l'$ (spin-singlet) doubly excited states.

RESULTS AND DISCUSSIONS

The results of the calculations for the B^{4+}-He system are presented in Table III and illustrated in Fig. 2. For most of the energy range in Fig. 2, capture into $2p$ B^{4+} states is the dominant process; capture into the $2s$ state is much weaker. A closer look at the results shows that the $2p_0$ and the $2p_1$ state (the quantization axis is the beam axis; the M quantum number is understood to combine both $|M|$ and $-|M|$ values) are populated about equally in the calculations, with the $2p_1$ state being slightly stronger. This indicates that rotational coupling on the outgoing part of the trajectory is very effective while the population of the final $2s$ state by radial coupling is weak.

Figure 2 shows that two-electron capture to doubly excited states is an important process over the whole of the considered energy range. Its summed cross section is never less than one-half of the cross section for single-electron capture to B^{3+} $2p$ states. Among the doubly excited states, the $2p^2(^1S)$ state is only very weakly popu-

TABLE III. Calculated cross sections (in 10^{-16} cm^2) for double-electron transfer to doubly excited $2l2l'$ states of B^{2+} in B^{4+}-He collisions. The M distribution for the population of ^1P and ^1D states is given for comparison with planned experiments [6].

Energy (keV/u)	$2s^2$	$2p^2(^1S)$	$2s2p(^1P0)$	$^1P1$	$2p^2(^1D0)$	$^1D1$	$^1D2$
1.5	1.41	0.040	0.177	0.096	0.110	0.050	0.068
2	1.100	0.024	0.185	0.163	0.125	0.058	0.116
3	0.896	0.039	0.308	0.150	0.113	0.143	0.093
7	0.670	0.043	0.454	0.292	0.134	0.217	0.058
15	0.479	0.026	0.257	0.292	0.204	0.334	0.068
30	0.277	0.021	0.218	0.189	0.258	0.316	0.067

lated; see Table III. Its population occurs at small-impact parameters of the order of 1 a.u. and lower, hence it should be assigned large uncertainties since the method of this paper is expected to be less reliable in the small-impact-parameter region. The population of the other states, however, occurs in the same range of impact parameters ($b \leq 4$ a.u.) that are important for single-electron capture. This is also true for the $2s^2$ B^{2+} state whose cross section becomes even larger than the cross section for $2p$ B^{3+} population at energies below 2 keV/u. From Fig. 2, and from the observation that transition *probabilities* for the $2s^2$ population are small (<0.3), it seems unlikely that this $2s^2$ B^{2+} state is populated by two successive single-electron transitions since otherwise the $2s$ B^{3+} state should be strongly populated as well. In other words: a single-electron-model description in conjunction with statistical arguments would fail to predict the population of the $2s^2$ B^{2+} state. One would rather be led to believe that the strong population of the $2s^2$ B^{2+} state at low energies is caused by those portions of the electron-electron interaction which cannot be accommodated in a single-electron model.

Experiments which determine absolute state-selective single- or double-capture cross sections are not available for this system. The relative populations, however, of the three doubly excited states and the M dependence for the nonspherical states, have been determined by measuring the angular distributions of ejected electrons [6]. In Table III we list the calculated double-capture cross sections and the M dependences for the $2s2p$ ^1P and the $2p^2$ ^1D states. These results are in good agreement with the recent measurements of Prior [6].

In Fig. 2 we show the apparent single-electron transfer cross sections measured by Iwai *et al.* [15] and Gardner *et al.* [16] by projectile-charge-state analysis. Both processes of single-electron and double-electron transfer lead to the change of the projectile charge state by one unit, in the case of double transfer to doubly excited states after stabilization of the projectile by autoionization. Hence the data in Fig. 2 should be compared to the sum of the calculated single- and double-transfer cross sections. The agreement is quite satisfactory. Also in Fig. 2 we show, at three energy points, the sum of calculated transfer cross sections from a calculation which includes the process of $n=3$ single capture. We do not give the details of results from that calculation which is numerically very demanding. We only note that the double-transfer cross sections from that calculation are about 30% lower than the numbers from the main calculation, the differences arising from the small-impact-parameter region. Uncertainties in the calculated state-specific cross sections due to limitations of the basis set may hence be estimated to be of the order of 50%, except for the $2p^2(^1S)$ state which is more uncertain.

The role of one-electron transfer as a mediator for two-electron transfer can also be illustrated in auxiliary dynamical calculations in which the one-electron transfer states are left out deliberately. In Fig. 3, the results of such calculations are shown. In discussing the curves in Fig. 3, it is well to remember that at small separation, all the basis states of an AO basis overlap and hence any interpretation should not attempt to deal with small effects. Keeping this in mind, it is still striking to observe that at low energies, the population of the $2s^2(^1P)$ and the $2s2p(^1P)$ B^{2+} states appears to be little influenced by the

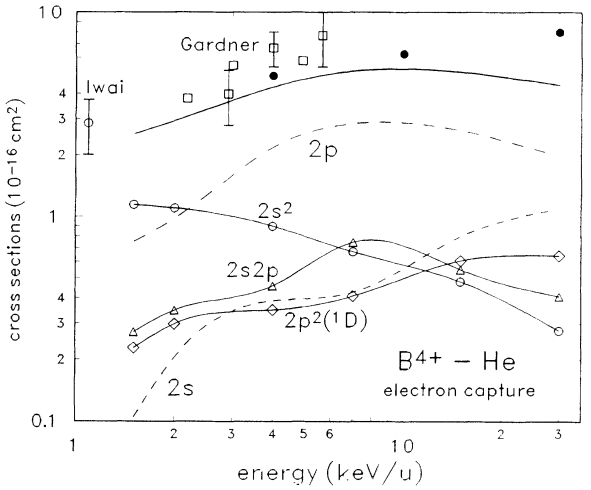

FIG. 2. Electron-capture cross sections in B^{4+}-He collisions. Shown are the calculated single-capture cross sections to B^{3+} $2s$ and $2p$ states (dashed lines) and the double-capture cross sections to $2s^2$, $2s2p$, and $2p^2(^1D)$ B^{2+} states (solid lines with open circles, triangles, and diamonds, respectively). The upper solid line denotes the sum of calculated single- and double-capture cross sections from this work; it is compared to the apparent single-capture cross sections measured by Iwai *et al.* [15] and by Gardner *et al.* [16] by projectile-charge-state analysis. The solid circles denote calculated total transfer cross sections from this work as does the solid curve but with the $n=3$ B^{3+} single-capture cross sections included.

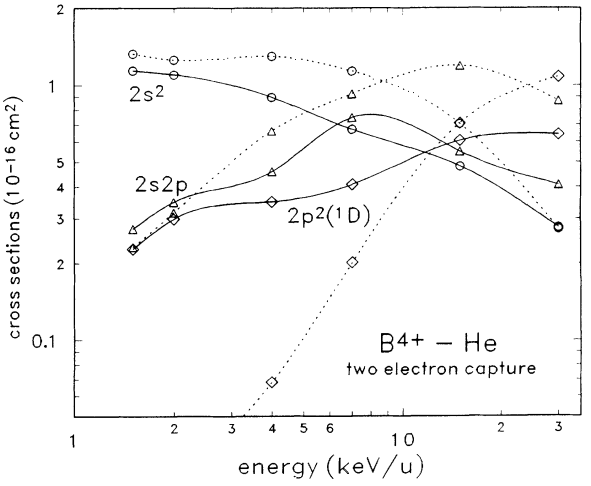

FIG. 3. Double-electron transfer cross sections calculated with a basis set that includes single-transfer states (solid lines) and with a basis set that does not include such states (dotted lines). Comparison of curves for a given final state shows to which degree that state is populated directly from the initial helium ground state or via the population of single-transfer states as mediators, see text.

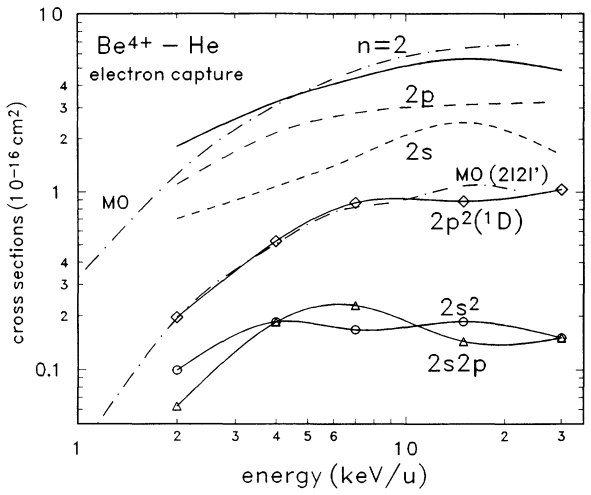

FIG. 4. Calculated electron-transfer cross sections in Be^{4+}-He collisions. Shown are the cross sections for transitions to the $2s$ and $2p$ Be^{3+} states from this work (dashed lines) and their sum (upper solid line). Cross sections from this work for transitions to $2p^2(^1D)$, $2s^2$, and $2s2p$ Be^{2+} doubly excited states are denoted by, respectively, diamonds, circles, and triangles. Summed single-electron cross sections and summed double-electron transfer cross sections from the calculations by Martin, Riera, and Yáñez [4] are displayed as dashed-dotted lines.

presence of the single-capture states. On the other hand, the population of $2p^2(^1D)$ B^{2+} states at low energies appears to proceed solely via the single-capture states as mediator.

In Fig. 4 we show the calculated electron-capture cross sections for the Be^{4+}-He collision system. The summed single-transfer cross section to the $n=2$ Be^{3+} shell agrees closely with the result reported by Martín, Riera, and Yáñez [4]. The transition to $2p$ states is seen in this work to be the strongest channel for this system like in the B^{4+}-He system, but here also the transition to $2s$ Be^{3+} states contributes to the total transfer cross section at low energy. Clearly, for a hydrogenic projectile (Be^{4+}) there is stronger mixing between l states than for a nonhydrogenic projectile (B^{4+}).

The calculated double-electron transfer cross sections are smaller than the cross sections for single transfer. The leading cross section as calculated in this work is to $2p^2(^1D)$ Be^{2+} states; it happens to agree fortuitously very closely with the total double-charge transfer which is reported in Ref. [4] to consist of mainly the $2s2p$ Be^{2+} component. The cross section to $2s2p$ states in this work is smaller and of the same order as the cross section to the $2s^2$ Be^{2+} state. Again, the $2p^2(^1S)$ Be^{2+} state is only weakly populated.

It is not easy to understand the discrepancy between the calculated double-electron transfer cross sections from this work and from the work by Martín, Riera, and Yáñez [4]. If one wanted to compare quantitative energy diagrams one would have to use the same stabilization methods as used in Ref. [4]. Also the coupling matrix elements in the AO-expansion method of this work would not be easily transformed into matrix elements between adiabatic states as used in Ref. [4]. One may be willing to accept a discrepancy at low energies on the argument that the adiabatic (MO) basis there is the better choice. The discrepancy, however, extends from the lowest energies up to 20 keV/u, and the important impact-parameter region here as in Ref. [4] is rather large (up to 4 a.u.). The question of substate population in double-electron transfer seems therefore to remain unsettled.

CONCLUSIONS

In this work we study the processes of single- and double-electron transfer in slow B^{4+}-He and in Be^{4+}-He collisions. In calculations within the semiclassical close-coupling description with atomic-orbital basis sets, we find that the population of specific doubly excited projectile states in double-electron transfer depends very sensitively on the particular system under consideration, e.g., on its core. For the Be^{4+}-He system, there is a discrepancy between the prediction of the strongest populated final state in double transfer, from this work and form the earlier work by Martín, Riera, and Yáñez, which is based on an adiabatic model. While the reason for this discrepancy is not clear, both studies agree on the total single-transfer cross section for this system, and on the observation that the single-transfer channel is the most important channel at all considered energies.

For the B^{4+}-He system this work shows that the process of double-electron transfer contributes a major portion to the total transfer cross section at low energies. There is no absolute experimental double-capture cross section available for comparison. However, the relative total capture cross sections among the doubly excited states and the relative M dependences within each state have been determined from the analysis of angular distributions of ejected electrons. The results of this work are in good agreement with the measurements. Furthermore, the sum of cross sections for single capture and double capture to doubly excited states are in good agreement with the apparent experimental single-capture cross sections. This overall consistency leads us to believe that the calculated single- and double-capture cross sections are sound, and that the present close-coupling approach using two-electron basis functions is capable of predicting reliable cross sections in slow ion-atom collisions if transitions occur at predominantly large internuclear separations. Still the discrepancy with the molecular close-coupling study for the Be^{4+}-He system is puzzling. More work would be needed for further clarification.

ACKNOWLEDGMENT

The work by C.D.L. has been supported in part by the U.S. Department of Energy, Office of Basic Energy Research, Division of Chemical Sciences.

[1] W. Fritsch and C. D. Lin, Phys. Rep. **202**, 1 (1991).
[2] M. Kimura, J. Phys. B **21**, L19 (1988).
[3] M. Kimura and R. E. Olson, Phys. Rev. A **31**, 489 (1985).
[4] F. Martín, A. Riera, and M. Yáñez, Phys. Rev. A **34**, 4675 (1986).
[5] R. A. Holt, M. H. Prior, K. L. Randall, R. Hutton, J. J. McDonald, and D. Schneider, Phys. Rev. A **43**, 607 (1991).
[6] M. Prior (private communication).
[7] H. Tawara, National Institute for Fusion Science Research Report No. NIFS-DATA-12, 1991 (unpublished).
[8] W. Fritsch and C. D. Lin, J. Phys. B **19**, 2683 (1986).
[9] C. E. Moore, *Atomic Energy Levels*, Natl. Bur. Stand. (U.S.) Circ. No. 35 (U.S. GPO, Washington, DC, 1971), Vol. 1.
[10] W. Fritsch and C. D. Lin, Phys. Rev. Lett. (1988).
[11] K. T. Chung and R. Bruch, Phys. Rev. A **28**, 1418 (1983).
[12] W. Fritsch and C. D. Lin, J. Phys. **15**, 1255 (1982).
[13] L. Opradolce, P. Valiron, and R. McCarroll, J. Phys. B **16**, 2017 (1983).
[14] K. Helfrich, Z. Phys. D **13**, 295 (1989).
[15] T. Iwai, Y. Kaneko, M. Kimura, N. Kobayashi, S. Ohtani, K. Okuno, S. Takagi, H. Tawara, and S. Tsurubuchi, Phys. Rev. A **26**, 105 (1982).
[16] L. D. Gardner, J. E. Bayfield, P. M. Koch, I. A. Sellin, D. J. Pegg, R. S. Peterson, M. L. Mallory, and D. H. Crandall, Phys. Rev. A **20**, 766 (1979).